A&A 492, 127–133 (2008)
DOI: 10.1051/0004-6361:200810622

Astronomy & Astrophysics

Carbonaceous dust in interstellar shock waves: hydrogenated amorphous carbon (a-C:H) vs. graphite

L. Serra Díaz-Cano and A. P. Jones

Institut d'Astrophysique Spatiale (IAS), Bâtiment 121, Université Paris-Sud 11 and CNRS, 91405 Orsay, France
e-mail: Anthony.Jones@ias.u-psud.fr

Received 16 July 2008 / Accepted 13 October 2008

ABSTRACT

Context. Observations of regions of the interstellar medium affected by shock waves indicate gas phase abundances of carbon that are close to solar. In quiescent regions less than half of the carbon is in the gas phase.
Aims. We propose that hydrogenated amorphous carbon (a-C:H), in its many guises, is the most probable form of carbonaceous grain material in the interstellar medium and study its erosion in shock waves.
Methods. We have used the physical properties typical of a-C:H materials, rather than graphite/amorphous carbon, to study a-C:H erosion during ion irradiation and fragmentation in grain-grain collisions. Using SRIM we study material-, surface- and size-dependent sputtering effects and introduce these effects into a shock model.
Results. We find significantly greater destruction for a-C:H, than for graphite, a result that brings the models into better agreement with existing observations of shocked regions of the ISM. Carbon grain erosion in shock waves therefore appears to be much more efficient than predicted by existing models.
Conclusions. Interstellar hydrogenated amorphous carbon dust is, apparently, rather easily destroyed in shocks and must therefore be more rapidly re-cycled and re-formed during its journey through the interstellar medium than previously-thought.

Key words. ISM: dust, extinction – shock waves – ISM: abundances – ISM: general – ISM: evolution

1. Introduction

Observational evidence from shocked regions in the interstellar medium (ISM) (Welty et al. 2002), in stellar jets in star-forming regions (Podio et al. 2006) and in the local interstellar cloud (Slavin 2008) shows high fractional abundances of gas phase carbon, i.e., ∼80−100% of the solar abundance, indicating that 60−100% of the carbon dust has been destroyed. For comparison, in quiescent regions of the diffuse ISM ∼40% of the available carbon is observed to be in the gas (Cardelli et al. 1996). Thus, for regions of the ISM shocked to velocities of the order of 50−150 km s^{-1} (Welty et al. 2002; Podio et al. 2006; Slavin 2008), it appears that the pre-existing carbon dust, whatever its original form, underwent major destruction. These observational results are clearly in contradiction with the predictions of the most recent graphite/amorphous carbon dust processing models (Tielens et al. 1994; Jones et al. 1994, 1996), which predict that ≤15% of the carbon dust will be eroded for shock velocities in the range 50−150 km s^{-1}.

It therefore appears that our current models for the nature of the carbonaceous dust in the ISM are probably in need of some revision. In the light of these critical observations a graphite/amorphous carbon model for interstellar carbon dust seems to be untenable.

Carbon stars are clearly important factories for the production of carbon-rich dust. There is now much observational evidence that this dust consists of hydrogenated amorphous carbon materials that form directly, and evolve compositionally, in the atmospheres of these evolved stars (e.g., Goto et al. 2003) and subsequently in the ISM (e.g., Jones 1990; Pino et al. 2008). Hydrogen incorporation and/or implantation into grains, in conjunction with photo-processing, in energetic regions of the ISM, e.g., HII regions, photo-dissociation regions and shock waves, would also likely pollute any pure carbon phase and lead to significant changes in its chemistry and structure. We therefore propose the range of materials collectively known as hydrogenated amorphous carbons (a-C:H) as a more realistic model for interstellar carbon dust (e.g., Jones 1990; Dartois et al. 2004, 2007; Dartois & Muñoz-Caro 2007; Pino et al. 2008).

In this paper we address the issue of carbon dust evolution in shock waves in the warm interstellar, inter-cloud, medium. In Sect. 2 we present a new description for interstellar carbon dust in terms of hydrogenated amorphous carbon, a-C:H, in Sect. 3 we present the results for the erosion of such grains in shocks using the derived physical properties of a-C:H, in Sect. 4 we discuss the impact of our new results for the evolution of interstellar carbon grains, and in Sect. 5 we present the conclusions of this study.

2. A new prescription for interstellar carbon dust

Current dust models use graphite, which is assumed to also be a good model for amorphous carbon, as the preferred material for interstellar carbon dust. This is principally because it can explain the extinction curve, has well-defined and well-measured physical properties and is relatively easy to model. A very recent update of the available SRIM code (Stopping and Range of Ions in Matter, version 2008.01, www.srim.org; Ziegler et al. 1985) has allowed us to re-evaluate some of the earlier graphite and amorphous carbon sputtering studies (Tielens et al. 1994; Jurac et al. 1998) and to extend these studies to a-C:H.

2.1. Graphite sputtering re-evaluated

We have used the latest version of the SRIM code (version 2008.01) to re-evaluate the sputtering yield of graphite as a function of the model input parameters and compare our yields with those calculated by Tielens et al. (1994) and Jurac et al. (1998). In the following sections we also take a closer look at the grain size dependence of the sputtering yields, as first investigated by Jurac et al. (1998).

The SRIM code uses a Monte-Carlo approach to calculate the effects of ion implantation into solids (and gases), to follow the collision cascades in a given solid and also to obtain sputtering yields as a function of the target material, the ion energy and the incident angle. The trajectories of the incident ions are followed through binary collisions with the target material atoms as they lose energy in each collision. The energy of the incident ions are followed as they displace the target atoms, heat the target and produce lattice vibrations. A target atom that receives enough energy to displace another target atom gives rise to a collision cascade and leads to vacancy formation. When the energy of an incident ion, or target atom, falls below that needed to displace target atoms the calculation stops.

The more recent releases of SRIM contain, among other important modifications, an updated treatment of the low energy ion-surface interactions. This is critical for our current study because it allows us to better model low-energy sputtering than was possible with earlier releases (e.g., as used by Jurac et al. 1998). The latest release does not necessarily give the same results as earlier versions and, as we shall show, enables a better comparison between experiment and model.

The input physical parameters for graphite, required by SRIM, that are now needed to re-produce the laboratory data for graphite sputtering (i.e., the surface and bulk atom displacement energies, U_0 and E_D, respectively, and the lattice energy, E_L) are given in Table 1 where they are compared with the the values used in the earlier study of Jurac et al. (1998). Figure 1 shows our calculated graphite sputtering yields for incident He and H ions compared to the laboratory data. We note that the input data values that we require to get a good fit to the experimental data (see Fig. 1), using the latest version of SRIM, are in good agreement with the measured values for graphite (e.g., Sun et al. 2005).

For our derived a-C:H sputtering yields we use the same approach and parameterisation as Tielens et al. (1994) except that in our analytical fits we adopt the following values: a mean a-C:H target atomic number $\langle Z_2\rangle = 4$ and atomic mass $\langle M_2\rangle = 7.6$, which were calculated using $\langle Z_2\rangle = [X_H Z_H + (1 - X_H)Z_C]$, $\langle M_2\rangle = [X_H M_H + (1 - X_H)M_C]$ and assuming an H atom fraction $X_H = N_H/(N_H + N_C) = 0.4$, where N_i is the number of atoms of element i (H or C). Note that for the range of a-C:H materials that we consider $\langle Z_2\rangle = 3.3$ to 5.0 and $\langle M_2\rangle = 6.0$ to 9.8, compared to 6.0 and 12.0, respectively, for graphite. Thus, the sputtering of hydrogen-poor a-C:H ($X_H = 0.2$) might be considered to approach that for graphite and the hydrogen-rich a-C:H ($X_H = 0.55$) be more susceptible to sputtering than our adopted "mean" a-C:H material. However, we note that the low density of a-C:H materials is critical and will mean that they are always more susceptible to sputtering than graphite.

We derive a value of −0.04 for the parameter K from a fitting of the SRIM-derived data to the analytical expression for the sputtering yield (Tielens et al. 1994, Eq. (4.13)). In this approach K is the only "truly free" parameter taking values from 0.1 to 0.65 for all of the materials considered by Tielens et al. (1994). These materials range from ice to solid Fe and the sputtering yields are therefore only weakly dependent on K. Finally, we adopt a typical threshold bulk carbon atom displacement energy of $E_{th} = 10$ eV (Sun et al. 2005).

Table 1. SRIM input parameters for graphite and a-C:H.

Material	ρ(g cm^{-3})	X_H	U_0(eV)	E_D(eV)	E_L(eV)
"old graphite"	–	0	3	11	2
graphite	2.26	0	7.4	28	3
a-C:H$_{(1)}$	1.5	0.2	4	10	3
a-C:H$_{(2)}$	1.4	0.4	4	10	3
a-C:H$_{(3)}$	1.3	0.55	4	10	3

Notes. ρ is the bulk material density (taken from Smith 1984 for a-C:H), X_H the hydrogen atomic fraction, U_0 is the surface atom binding energy, E_D bulk atom displacement energy and E_L the lattice energy. The values used by Jurac et al. (1998) are here designated as "old graphite".

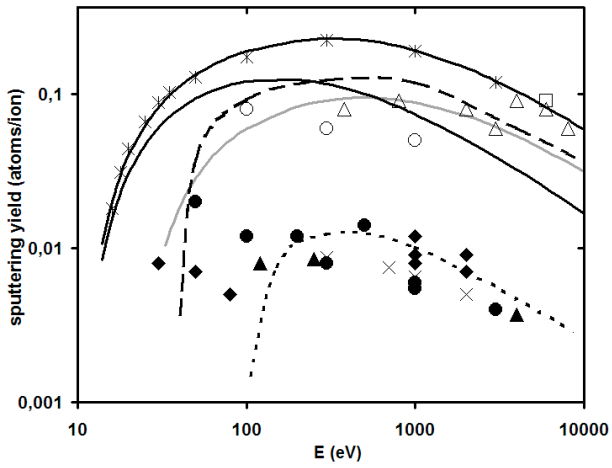

Fig. 1. Our SRIM-calculated sputtering yields for incident He [H] ions on graphite (long-dashed) [dotted] compared with the Tielens et al. (1994) He sputtering yield for graphite/amorphous carbon (solid grey). Also shown are the new SRIM-derived He [H] sputtering yields for a-C:H (upper black curve) [lower black curve] fitted to the SRIM data for He (asterisks, SRIM H data not shown) and fitted with the Tielens et al. (1994) formalism. The experimental sputtering yields for graphite (He, open symbols, and H, filled symbols, respectively) are also shown, these data are taken from Jurac et al. (1998) and Tielens et al. (1994), see references therein.

2.2. Amorphous hydrogenated carbon (a-C:H) sputtering

Given that a large fraction of the carbon dust in the ISM is likely to be in the form of a-C:H-like materials, graphite is then probably not the most abundant component of interstellar carbon dust. In any event, even if all the carbonaceous dust formed around evolved stars were to be in graphitic form, an unlikely scenario, it would be modified by ion irradiation (e.g., Banhart 1999; Mennella et al. 2003; Mennella 2006) in the ISM to an amorphous form implanted with heteroatoms, principally H atoms. We now investigate hydrogenated amorphous carbons as an alternative material for interstellar carbon dust.

In order to model a-C:H we have calculated its physical properties using the same approach as Tielens et al. (1994). In the absence of suitable constraints we adopt the same s parameter as for graphite. For the sound speed, c_0, of a-C:H we estimate a value of 1 km s^{-1} based on $c_0 = \sqrt{(B/\rho)}$, where B is the bulk modulus, here we have assumed $B = 1.4 \times 10^{10}$ dyne cm^{-2} and $\rho = 1.4$ g cm^{-3} (Table 1). In determining the vaporisation

Table 2. Comparison of the physical parameters for graphite and a-C:H.

	Fragmentation		Vaporization	
Parameter	Graphite	a-C:H	Graphite	a-C:H
ρ_0 [g cm^{-3}]	2.2	1.4	2.2	1.4
c_0 [km s^{-1}]	1.8	1.0	1.8	1.0
s	1.9	1.9	1.9	1.9
$P_{\rm th}$ [dyne cm^{-2}]	0.4×10^{11}	0.2×10^{11}	5.8×10^{12}	2.8×10^{12}
$\varepsilon_{\rm v}$ [erg g^{-1}]	1.8×10^{9}	0.75×10^{9}	6.4×10^{11}	5.2×10^{11}
$v_{\rm th}$ [km s^{-1}]	1.2	0.8	23	20
$E_{\rm b}$ [eV]	0.02	0.01	8	6.5

Note. Physical parameters for fragmentation and vaporization for a-C:H (this work) and for graphite/amorphous carbon (Tielens et al. 1994). c_0 is the sound speed, s is a dimensionless parameter, $P_{\rm th}$, ε_v and $v_{\rm th}$ are the relevant threshold pressure, energy density and velocity, respectively. $E_{\rm b}$ is the binding energy.

parameters for a-C:H the binding energy, $E_{\rm b}$, is the defining parameter and $P_{\rm th}$, ε_v and $v_{\rm th}$ can be derived from it. We adopt the following values for the aliphatic (C-C) and olefinic (C=C) bond energies, 3.6 eV and 6.3 eV, respectively, equivalent to a relatively aliphatic-rich a-C:H, and calculate the binding energy $E_{\rm b} = E_{\rm C-C} + 0.5E_{\rm C=C} = 6.5$ eV. For the calculation of the fragmentation parameters, ε_v, $v_{\rm th}$ and $E_{\rm b}$, it is $P_{\rm th}$ that is the defining parameter. Given the lack of experimental data for a-C:H we estimate $P_{\rm th} = 0.02 \times 10^{12}$ dyne cm^{-2} for fragmentation by adopting the same scaling as for the graphite vaporisation and fragmentation threshold pressures. We compare our calculated properties of a-C:H with those of graphite in Table 2.

We have studied the sputtering yields for the three a-C:H materials presented in Table 1 using SRIM in order to investigate the sensitivity of the results to the physical properties of a-C:H. We find that the sputtering yield for all three of our a-C:H materials is essentially the same. Figure 1 compares the sputtering yield of our a-C:H$_{(2)}$ (Table 1) with that for graphite (this work and Tielens et al. 1994). An increase in the sputtering yield of a-C:H, with respect to graphite, by a factor of at least two is found because of the lower material densities and the lower binding energies for a-C:H. The difference in the threshold energies in Fig. 1 is, principally, a function of the assumed bulk atom displacement energy $E_{\rm D}$.

2.3. Size, angle and surface erosion effects

The dependence of the a-C:H sputtering yield on the incidence angle, θ, is shown in Fig. 2. The lower densities of a-C:H lead to a deeper penetration of the ions, with respect to graphite, which results in them having enough energy to produce an enhanced destruction of the material surface. We note that a-C:H is therefore more sensitive to sputtering at large incidence angles than graphite (see Fig. 2). With respect to the experimental results SRIM is known to underestimate the sputtering at angles between about 30° and 50° (Jurac et al. 1998). We therefore expect that the yield between these angles will be larger than is found with SRIM and a modification of the angle-averaged sputtering yield is therefore needed so as to not underestimate the a-C:H yields. The angle-averaged sputtering yield that we find for a-C:H is:

$$\langle Y_{\rm a-C:H} \rangle_\theta = 4\, Y_{\rm a-C:H}(\theta = 0). \quad (1)$$

Note that the factor of four that we find here for a-C:H, i.e., the enhancement with respect to the normal incidence case, $Y_i(\theta = 0)$, is a factor of two higher than that typically assumed for other

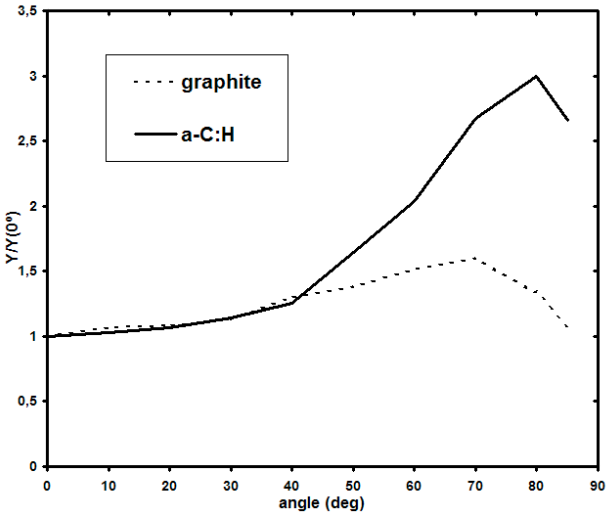

Fig. 2. Sputtering yield for 100 eV He ions incident on a-C:H and graphite as a function of the incident angle (0° represents normal incidence). An increase in the angular dependence of the sputtering yield, in comparison with graphite, is clearly indicated.

materials, including graphite (e.g., Tielens et al. 1994). In our a-C:H thermal sputtering calculations we have therefore increased the yields by a factor of four to take into account the factor of two enhancement, in each case, for the angle-dependent and material-dependent sputtering of a-C:H with respect to graphite.

We investigate an important physical effect that was first proposed and studied by Jurac et al. (1998), namely a size-dependence of the material sputtering yields. They proposed that the sputtering destruction of grains is increased for the smallest grains where the grains are about same size as the dimensions of the collision cascades. In this case the destruction is enhanced over the entire grain surface. However, this may affect only a small fraction of the total grain mass because most of the grain mass in a typical ISM dust size distribution is in the largest grains (see later).

In order to reproduce the effects of this size-dependent target atom sputtering with SRIM we ran into one of its current limitations, i.e., that SRIM does not provide the detailed positions and origins of the displaced target atoms. (Jurac et al. (1998) overcame this problem by completely re-formulating the available version of the code, which was known as TRIM at that time.) As there is no access to the displaced target atom final positions, but SRIM does provide the implanted incident ion positions, we were able to use simple scaling arguments to achieve our aims. That a relationship between the distributions of the implanted incident ions and the displaced target atoms exists is based upon the fact that the maximum in the position of the displaced target atoms occurs where the incident ions lose most of their energy. The three-dimensional form of the two distributions must therefore be similar. We found that, for the energies of interest to us, a scaling factor of ~0.7 allowed us to convert the implanted ion distribution peak positions and widths to that of the equivalent displaced target atom distributions. This then enabled us to solve the problem of the displaced atom distribution by a simple scaling between the implanted and displaced atom distributions. The derived distribution of the displaced atoms was integrated over a spherical volume, defined by the grain radius, in order to calculate the sputtering loss from finite-sized particles. The effects of incident ions implanted further than twice the grain size were not considered in the integration because the first collision occurs

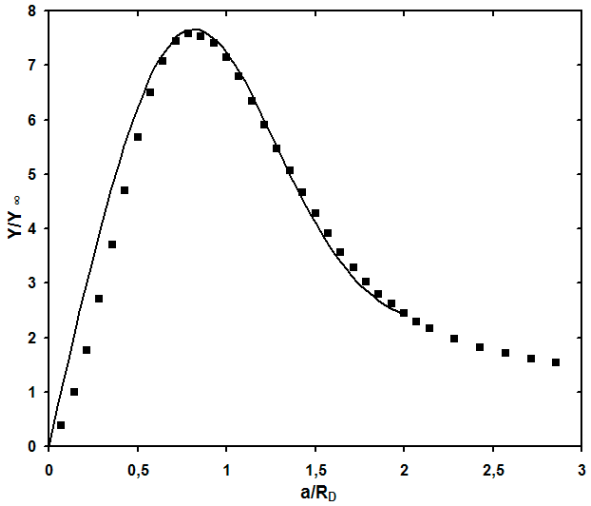

Fig. 3. Sputtering yield, Y, normalized to the yield for a semi-infinite surface at normal incidence, Y_∞, for a-C:H as a function of the ratio of the grain radius, a, to the peak of the implanted ion distribution, R_D. The squares show our SRIM results for a-C:H and the solid line shows the analytical fit to these data that we adopt in our grain sputtering calculations.

outside the grain volume and they can therefore be considered as transmitted ions.

The enhancement in the sputtering yield for small grains is shown in Fig. 3. An increase in the sputtering yield is evident for the grains when R_D is of the same order as the grain radius. This arises because the collision cascades result in sputtering from most of the grain surface. The drop-off at low values of a/R_D is due to the fact that the incident ions traverse the grain, and produce less sputtering, as a/R_D decreases. The SRIM data does not follow a simple analytical function, so we have fitted it using a combination of gaussian functions to reproduce the asymmetrical wings in the data.

2.4. The processing of a-C:H in shock waves

In our previous work (Jones et al. 1994, 1996) we considered the dynamics and processing of a Mathis et al. (1977) size distribution of carbon grains assumed to be of graphite/amorphous carbon composition. The processing of these grains by inertial and thermal sputtering in ion-grain collisions and by vaporisation and shattering in grain-grain collisions was taken into account for all the considered grain sizes. In this work we have adopted the same approach but use the physical parameters for a-C:H rather than graphite for the carbon grains.

When grains enter a shock they become charged and gyrate around the compressed magnetic field lines. This leads to relative gas-grain velocities and hence to collisions with the gas (and with other grains). Collisions with the gas lead to a coupling of the particles to the gas and therefore a decrease in the relative gas-particle velocity. However, these same collisions with the gas also lead to the removal of atoms from the particle if the relative velocites are larger than the given threshold for an erosional process (e.g., Tielens et al. 1994), for sputtering in ion-particle impacts this occurs at velocities greater than a few tens of km s^{-1}.

In determining the processing of grains in shock waves it is the relative gas-grain velocity profile through the shock that determines the level of processing. In calculating the relative ion-grain velocity through the shock we use the same approach as in our previous work (Jones et al. 1994, 1996). The grains are injected into the shock with 3/4 of the shock speed and their trajectory is then calculated self-consistently throughout their coupling to the gas, to the point at which the relative gas-grain velocity becomes negligible. The velocity calculation includes the effects of the direct drag with the gas due to atom and ion collisions and the drag due to the ion-charged grain interaction in the post-shock plasma. All the relevant expressions and assumptions for the calculation of the grain velocity, betatron acceleration and grain charge are fully described in McKee et al. (1987). Note that in this work we adopt the McKee et al. (1987) grain charge scheme and therefore implicitly assume that a-C:H grains follow the same charging processes. This may not indeed be the case, as pointed out by Jurac et al. (1998), but in the absence of any suitable studies on a-C:H grain charging processes we leave detailed studies of this to a later date.

We introduce this newly-characterised a-C:H material into our shock code in order to study the evolution of a-C:H dust grains and their destruction in interstellar shock waves in the warm ionised interstellar medium as per our previous studies (Jones et al. 1994, 1996). In our study we include the effects of the enhanced sputtering yields for a-C:H, with respect to graphite, and the angle- and size-dependent effects described above. For the size dependent effect we use the data described in Fig. 3 in order to account for the erosion of all carbon grains.

3. Results

Figures 4 and 5, and Table 3 allow us to directly compare our new results with those of our previous models without (Jones et al. 1994) and with Jones et al. (1996) the effects of carbon grain fragmentation in grain-grain collisions. From these data we can see that there is increased erosion of a-C:H grains, with respect to graphite/amorphous carbon, by a factor of about 3–4 compared to our previous results. This increase is apparent for all of the shock velocities considered (V_s = 50–200 km s^{-1}), except in the case of the fastest shock considered, v_s = 200 km s^{-1}, where we now find a complete destruction of the a-C:H grains primarily due to the effects of thermal sputtering. This rather robust result is independent of the inclusion of fragmentation into the grain processing scheme.

As described earlier we include size-dependent erosion effects into our shock code. However, we note that this effect could perhaps also be considered as a surface effect because of the enhancement of surface sputtering at low incidence angles (see Fig. 2). With the inclusion of the size-dependence into the sputtering erosion scheme we find that there is a slight enhancement in grain erosion for a characteristic grain size for each shock velocity. The peak of the effect corresponds to the maximum in Fig. 3. However, in essence, only a small fraction of the total grain mass experiences enhanced destruction due to this size effect when this is integrated over the full grain size and velocity distribution through the shock. The increase in the erosion due to the inclusion of the size effect is only of the order of 1% of the total carbon dust mass. This small effect is perhaps much weaker than that expected by Jurac et al. (1998) and is principally due to the fact that the size-dependent erosion must turn over at some point as the energetic ions traverse the grains and produce little erosion, a limitation that was not included in this earlier work.

Figure 6 compares our fragmentation results for graphite/amorphous carbon and a-C:H, for an assumed initial Mathis et al. (1977) size distribution. As can be seen the effect of fragmentation on a-C:H grains is much reduced, This reduction is due principally to the lower peak a-C:H grain

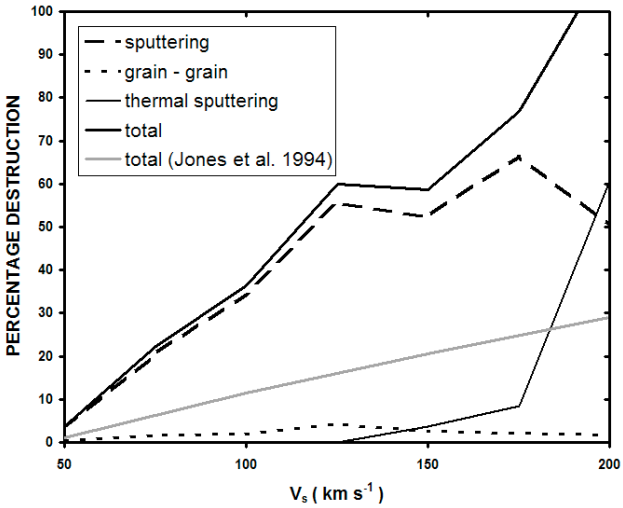

Fig. 4. Destruction of a-C:H grains as a function of the shock velocity calculated, in the absence of fragmentation in grain-grain collisions, as per Jones et al. (1994) (thick solid line). We show the effects of inertial sputtering (long-dahsed line), thermal sputtering (thin solid line), vaporisation in grain-grain collisions (short-dashed line) and our previous results (total destruction, solid grey line).

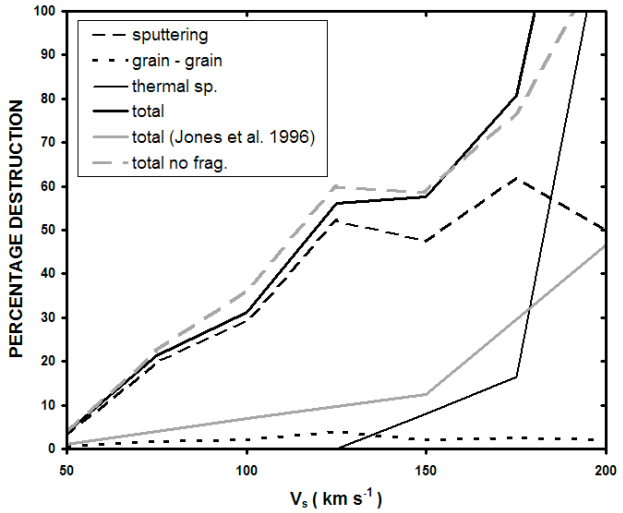

Fig. 5. Destruction of a-C:H grains as a function of the shock velocity calculated with the inclusion of fragmentation in grain-grain collisions as per Jones et al. (1996). The line types are the same as in Fig. 4. We also show the total for the case without fragmentation from Fig. 4 (grey dashed line).

velocities and reduced gas-grain coupling time-scales arising from the lower density of a-C:H (1.4 g cm^{-3}) with respect to graphite (2.26 g cm^{-3}).

4. Discussion

Welty et al. (2002) used near-UV spectra from the *Hubble Space Telescope* GHRS to measure the abundances and determine the physical conditions within the ISM in high velocity (HV, -105 km s^{-1} $\lesssim V_\odot \lesssim -65$ km s^{-1}) and intermediate velocity (IV, -60 km s^{-1} $\lesssim V_\odot \lesssim -10$ km s^{-1}) gas toward the star ζ Ori. They find Al, Si and Fe depletions indicative of about 10% silicate dust destruction, which is consistent with the latest models for silicate grain destruction (Jones et al. 1994, 1996). However, for carbon they find near-solar gas phase abundances indicating

Table 3. Percentage destruction for carbonaceous grains in shocks.

V_S (km s^{-1})	50	75	100	125	150	175	200
No fragmentation							
JTHM94	1.1	–	11.5	–	20.5	–	29
This work	3.6	22.2	36.2	59.7	58.5	76.8	100
Fragmentation included							
JTH96	1.1	–	7.0	–	12.4	–	46.7
This work	3.8	21.4	31.3	56.1	57.7	80.9	100

Note. Graphite/amorphous carbon grains without fragmentation (JTHM94, Jones et al. 1994) and with fragmentation (JTH96, Jones et al. 1996). Results for a-C:H (This work).

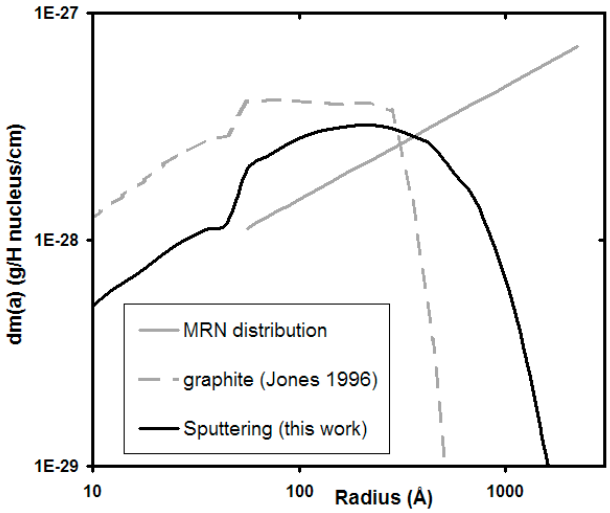

Fig. 6. The effects of a-C:H grain fragmentation and erosion in a 100 km s^{-1} shock for an initial Mathis et al. (1977) grain size distribution (solid grey line), for a-C:H carbon grains (this work, solid black line) and our previous results for graphite (grey dashed line; Jones et al. 1996).

60–70% carbon dust destruction. Podio et al. (2006) used optical and infrared diagnostics to probe the dust erosion in Herbig-Haro jets in the Orion and Vela star forming regions. They find substantial, but incomplete, Ca- and Fe-bearing dust destruction (0–70% and 90% in the gas for Ca and Fe, respectively). They also find that carbon is not depleted in these shocks with respect to solar abundances, i.e. carbon dust is essentially completely destroyed. Frisch et al. (1999) and Slavin (2008) studied the nature of the dust in the local interstellar wind and cloud and find that the silicate grain elemental depletions (Si, Mg and Fe) are consistent with the local cloud having been shocked to a velocity of the order of 150 km s^{-1}. However, Slavin (2008) finds that the gas phase carbon abundance in the local cloud is at least solar, indicating the complete destruction of the carbon grains in the local ISM that was shocked by the supernova event that gave rise to the local bubble structure (Frisch et al. 1999).

In adopting an a-C:H model for interstellar carbon dust, and abandoning graphite, we find that we are able to better explain the general trends indicated in the observational data (Frisch et al. 1999; Welty et al. 2002; Podio et al. 2006; Slavin 2008), i.e., that a large fraction of the carbon dust in the ISM is destroyed by the passage of shocks with velocities of the order of 50–150 km s^{-1}. Our results for an a-C:H carbon dust model for a shock velocity of 100 km s^{-1}, i.e., ≡70–80% carbon in the gas (Table 3), are in rather good agreement with the observational results (Welty et al. 2002; Podio et al. 2006; Slavin 2008), and

in much better agreement than the results of the previous models using graphite as the solid carbon phase (Jones et al. 1994, 1996). These results and the observational data indicate that essentially all of the carbon dust is destroyed in such energetic regions.

Our results are, however, probably still something of an underestimate of the carbon dust erosion because we have here neglected the chemical sputtering effects of hydrogen in our calculations. SRIM does not allow this to be taken into account but comparison of the SRIM results for graphite with experiment (Fig. 1) shows that at low proton irradiation energies the erosion is enhanced with respect to the SRIM predictions. Also, in SRIM it is not possible to properly take into account the effects of previous irradiation and therefore there is no irradiation "history", which in the case of a-C:H materials could play a very important role in rendering the material more "erode-able".

Using the same method as in our previous works (Jones et al. 1994, 1996) we have calculated the lifetime for hydrogenated amorphous carbon grains in the ISM. We find a carbon dust lifetime of the order of 1.7×10^8 yr, as compared to the value of 6.3×10^8 yr derived by Jones et al. (1996). This should be compared to the typical dust injection lifetime of 3×10^9 yr. However, in order to preserve a significant fraction (≈90%) of the carbon dust formed around evolved stars (i.e., stardust) in the ISM would require a dust lifetime of the order of 10^{10} yr (e.g., Jones et al. 1996), i.e., a discrepancy of ≈60 between the required lifetime and the shock processing-derived lifetime.

Can we perhaps preserve dust in the densest regions of the ISM? Star formation actively disrupts clouds on time-scales of the order of 3×10^7 yr due to the photo-dissociation and photo-ionisation of diffuse and molecular clouds by massive stars (e.g., McKee 1989). In this case, as mentioned above, at most only 10% of the stardust ejected into the ISM from evolved stars can escape processing in shocks and be preserved "intact" in the ISM (Jones et al. 1994, 1996). We therefore, seemingly, cannot protect a large fraction of the dust from the effects of shock waves by hiding it in the dense phases of the ISM.

The higher destruction rate for a-C:H grains, with respect to graphite, therefore has major consequences for the evolution of carbon dust in the ISM. It implies that the cycling time-scale for carbon dust is much shorter than that for silicate grains, and much shorter than that implied by our earlier results for carbon dust (Jones et al. 1996). We may therefore need to focus our attention on how the structure of the ISM phases, and the cycling of matter between those phases, could perhaps help in explaining this rapid cycling requirement. Clearly, we require an efficient mechanism for the re-formation of carbonaceous dust if we are to explain observations that indicate that, in quiescent regions of the ISM, typically half of the available carbon is in the form of dust (e.g., Cardelli et al. 1996).

Based on a series of catalytic-type reaction experiments Nuth et al. (2008) discuss an interesting mechanism for the formation of macro-molecluar, carbonaceous materials from CO and H_2 on the surfaces of amorphous iron and magnesium silicates and pure silica smokes. This appears to be a viable process for the formation of organic materials under primitive solar nebula conditions. If this process could also operate in the lower density ISM then it might provide a viable route to hydrogenated amorphous carbon grain re-formation. However, it might be that the accretion process in the ISM begins before the formation of CO and H_2 with the re-accretion of the atomic components (H, C, O, etc.) onto the residual grain surfaces after having been sputtered into the gas in shocked regions. In this case we then also have to explain the chemically-segregated formation of hydrocarbon and silicate grain phases in a gas composed, predominantly, of the condensible elements H, C, O, Si, Mg and Fe.

Our model for the nature of a-C:H materials is, of course, dependent upon their measured properties, many of which are not currently available in the literature. The results that we present should therefore be considered as representative of the range of materials that come under the umbrella of a-C:H, i.e., we do not prescribe an absolute sputtering rate. However, we have shown that taking into account the likely properties of a-C:H leads to such large differences, compared to graphite/amorphous carbon, that a serious re-consideration of previous results is warranted.

5. Conclusions

Using what we consider to be a realistic model for interstellar carbon dust, i.e., hydrogenated amorphous carbons (a-C:H), we have investigated the effects of a-C:H dust processing in interstellar shocks in the warm inter-cloud medium of the ISM. We believe that a-C:H is a more reasonable model for interstellar carbon dust because, even if a large fraction of carbon dust were to be injected into the ISM in a graphitic form, it is unlikely that it could remain as such when subjected to the effects of erosion and ion irradiation in shock waves (principally by H^+ and He^+).

In our study we have included a-C:H grain composition, size, surface and fragmentation effects using newly-derived physical parameters for a-C:H. We find that size effects are not particularly important and that our results are not sensitive to the assumed a-C:H composition for the carbon dust. The results for all of the a-C:H materials that we consider here are essentially identical. The biggest difference is in comparison with graphitic carbon dust because of the significantly lower density of a-C:H materials compared to graphite.

We find that for all shock velocities the a-C:H carbon grain erosion is, at least, a factor of three higher than for the graphite grain model, except for the highest shock velocities considered here where carbon grain destruction is complete due to the effects of thermal sputtering in the hot post-shock gas. Our new data appear, qualitatively at least, to agree much better with the observations of approximately solar gas phase carbon abundances in shocked regions of the ISM. However, the sputtering yields, and hence the degree of carbon grain destruction, that we derive are almost certainly lower limits because we neglect the possibly important effect off chemical sputtering by protons.

The fragmentation of a-C:H grains turns out to be less important than for graphitic grains and leads to the better preservation of the larger grains. Although the effect is still rather dramatic but less so than for graphite. Our results for the degree of a-C:H grain destruction are rather independent of the inclusion of fragmentation into the carbon grain processing scheme and are therefore rather robust.

We derive new carbon dust lifetimes in the ISM of the order of $\sim 2 \times 10^8$ yr, which are a factor of about 3 shorter than our previous estimates. This is a factor of about 60 shorter than the time-scale that would be required to preserve a large fraction (≈90%) of carbon stardust in the ISM. These time-scale discrepancies appear to further complicate the picture of our current view of carbon dust evolution in the ISM. In order to explain the observations, that of order half of the carbon is in dust in the quiescent ISM, we need to invoke an efficient carbon dust re-formation scenario in which a form of hydrocarbon dust (a-C:H-like) is re-accreted in some phase of the ISM onto the surfaces of remnant interstellar carbon (or possibly silicate) grains.

Given the apparent importance of fragmentation in shock waves it may be that the re-accretion of eroded dust atoms in

quiescent regions of the ISM is aided by the relatively large surface area that would be provided by the small fragments surviving post-shock. Additionally, we suggest that stochastic heating effects might aide any chemical selection effect that would tend to favour carbon (Si, Mg, Fe and O) atom sticking to remnant carbon (silicate) "seed" grains. In this case the stronger "like-to-like" chemical bonding might increase the probability of C atom retention on carbon surfaces during stochastic heating events and, likewise, Si, Mg, Fe and O atom retention on silicate/oxide surfaces.

Acknowledgements. We wish to thank Pierre Guillard, Elisabetta Micellota, Vincent Guillet and Guillaume Pineau des Forêts for interesting discussions on carbon dust in shocks and the use of the SRIM code. We also wish to thank the referee, Joe Nuth III, for a useful exchange of ideas.

References

Banhart, F. 1999, Rep. Prog. Phys., 62, 1181
Cardelli, J., Meyer, D. M., Jura, M., & Savage, B. D. 1996, ApJ, 467, 334
Dartois, E., & Muñoz-Caro, G. M. 2007, A&A, 476, 1235
Dartois, E., Muñoz-Caro, G. M., Deboffle, D., & d'Hendecourt, L. 2004, A&A, 423, L33
Dartois, E., Geballe, T. R., Pino, T., et al. 2007, A&A, 463, 635
Frisch, P. C., Dorschner, J. M., Geiss, J., et al. 1999, ApJ, 525, 492
Guillet, V., Pineau des Forêts, G., & Jones, A. P. 2007, A&A, 476, 263
Goto, M., Gaessler, W., Hayano, Y., et al. 2003, ApJ, 589, 419
Jones, A. P. 1990, MNRAS, 247, 305
Jones, A. P., Tielens, A. G. G. M., Hollenbach, D. J., & McKee, C. F. 1994, ApJ, 433, 797
Jones, A. P., Tielens, A. G. G. M., & Hollenbach, D. J. 1996, ApJ, 469, 740
Jurac, S., Johnson, R. E., & Donn, B. 1998, ApJ, 503, 247
Mathis, J. S., Rumpl, W., & Nordsieck, K. H. 1977, ApJ, 217, 425
McKee, C. F. 1989, in Interstellar Dust, ed. L. J. Allamandola, & A. G. G. M. Tielens (Dordrecht: Kluwer), IAU Symp., 135, 431
Mennella, V. 2006, ApJ, 647, L49
Mennella, V., Baratta, G. A., Esposito, A., Ferini, G., & Pendleton, Y. J. 2003, ApJ, 587, 727
McKee, C. F., Hollenbach, D. J., Seab, G. C., & Tielens, A. G. G. M. 1987, ApJ, 318, 674
Nuth III, J. A., Johnson, N. M., & Manning, S. 2008, ApJ, 673, L225
Pino, T., Dartois, E., Cao, A.-T., et al. 2008, A&A, in press
Podio, L., Bacciotti, F., Nisini, B., et al. 2006, A&A, 456, 189
Slavin, J. D. 2008, SSRv, submitted [arXiv:0804.0161v1]
Smith, F. W. 1984, J. Appl. Phys., 55, 764
Sun, L. T., Gong, J. L., Wang, Z. X., et al. 2005, Nuc. Inst. Meth. in Phys. Res. B, 228, 26
Tielens, A. G. G. M., McKee, C. F., Seab, G. C., & Hollenbach, D. J. 1994, ApJ, 431, 321
Welty, D. E., Jenkins, E. B., Rayomnd, J. C., & Mallouris, C. 2002, ApJ, 579, 304
Ziegler, J. F., Biersack, J. P., & Littmark, U. 1985, The Stopping and Range of Ions in Matter, ed. J. F. Ziegler (Pergammon Press)